Negative pion interactions with ^{19}F, ^{27}Al, and ^{51}V near the $\Delta(1232)$ resonance*

B. J. Lieb, W. F. Lankford, and S. H. Dam†
Department of Physics, George Mason University, Fairfax, Virginia 22030

H. S. Plendl
Department of Physics, Florida State University, Tallahassee, Florida 32306

H. O. Funsten and W. J. Kossler
Department of Physics, College of William and Mary, Williamsburg, Virginia 23185

V. G. Lind
Department of Physics, Utah State University, Logan, Utah 84322

A. J. Buffa
Department of Physics, California Polytechnic State University, San Luis Obispo, California 93401

(Received 25 September 1975; revised manuscript received 15 April 1976)

Prompt γ rays from π^- interactions with ^{19}F, ^{27}Al, and ^{51}V near the $\Delta(1232)$ resonance were detected. Deexcitation γ rays from residual nuclei formed by single and multiple nucleon removal and by inelastic and charge exchange scattering were identified, and cross sections for excitation of residual states were determined. Nuclear recoil momenta were determined from observed Doppler broadening. Where possible, the cross sections were corrected for γ feeding from higher states. The results are compared with the results of previous experiments and of intranuclear cascade/evaporation code calculations.

[NUCLEAR REACTIONS ^{19}F, ^{27}Al, $^{51}V(\pi^-, X\gamma)$, $E_{av} \approx 230$ MeV, measured relative γ-ray yields at $\theta = 90°$, calculated σ, nuclear recoil momenta.]

I. INTRODUCTION

In several recent experiments,[1-16] meson-nucleus reactions resulting in single or multiple nucleon removal have been investigated. Because of beam intensity and resolution limitations, the reactions were studied by indirect means such as detection of prompt deexcitation γ rays from residual nucleus bound states[1-9] or of β activity from residual nucleus ground states.[10-16] The prompt γ ray studies have resulted in a wealth of information on reaction channels leading to the formation of residual states which would be unattainable by activation or other methods. However, ground state formation without prior excitation and γ deexcitation of an excited state cannot be observed by this method, nor can the extent to which γ feeding from higher states contributes to the cross section be determined for all excited states. Furthermore, the identity of the outgoing meson, nucleons, or nucleon clusters cannot be established by prompt γ ray detection alone.

Previous prompt γ ray studies have concentrated on even-even target nuclei from ^{12}C to ^{60}Ni. High cross sections were found for the production of residual nuclei corresponding to the removal of multiples of two neutrons and two protons (generally referred to as equivalent α particles, since outgoing particles were not detected in these experiments). Tentative evidence for interaction of stopped π^- with α clusters in several nuclei ranging from Li to Pb was obtained by Castleberry *et al.*[17] who determined the angular correlation of the resulting neutrons and tritons. Actual α particles from 70 MeV π^- interactions with ^{27}Al were observed recently by Doron *et al.*[18] with an extrapolated total cross section of ~100 mb. Single and multiple removal of equivalent α particles with large cross sections has also been observed with 100 MeV protons on ^{56}Fe and ^{58}Ni (Ref. 19) and with 200 MeV pions on ^{58}Ni and ^{60}Ni.[9] The results reported in Refs. 18 and 19 have been reproduced reasonably well by intranuclear cascade/evaporation calculations (cf. Sec. IV D) in which α particle removal was allowed only in the evaporation phase.

The large equivalent α particle removal cross sections observed in the prompt γ ray experiments on even-even targets may have been enhanced by γ branching systematics. While γ transitions in even-even residual nuclei cascade predominantly to the ground state through the lowest 2^+ level, there is no corresponding level through which most γ rays cascade in odd nuclei. Hence,

a γ ray yield from the lowest 2^+ level in a residual even-even nucleus that is larger than the yield from the lowest level in a residual odd nucleus does not necessarily correspond to a larger cross section for formation of the even-even nucleus, unless corrections for feeding from higher levels have been made.

In the present work, prompt γ rays from π^- interactions with the odd-mass target nuclei ^{19}F, ^{27}Al, and ^{51}V were studied. Results for single and multiple nucleon removal and for inelastic and charge exchange scattering are presented and compared with the results of recent pion scattering, reaction and absorption experiments on these targets, and also with the results of the experiments on even-mass targets. The extent to which single nucleon removal reactions may be quasifree is examined by comparing the present results with experimentally determined spectroscopic factors. The cross sections determined in the present work are also compared with the predictions of a model in which an initial intranuclear cascade is followed by evaporation. Some of the experimental results have been reported in preliminary form in Refs. 4, 20, and 21.

II. EXPERIMENT

The experiment was performed at the SREL synchrocyclotron (The Space Radiation Effects Laboratory is supported by NSF, NASA, and the Commonwealth of Virginia) using the nominal 240 MeV π^- beam. The pions were produced by protons on an internal carbon target, then deflected out of the cyclotron by its fringing field, focused by a quadrupole pair, and momentum selected by a bending magnet.

The experimental geometry is shown in Fig. 1. The beam passed through two 10 cm $\times$ 10 cm $\times$ 0.65 cm scintillation counters (labeled No. 1 and No. 2) and was then incident on the target. The beam intensity as determined by this counter telescope was approximately 4×10^5 particles/sec, including a lepton contamination of $(20 \pm 5)\%$ as determined by time of flight. Isotopically unseparated targets of LiF (2.75 g/cm^2), ^{27}Al (13.5 g/cm^2), and ^{51}V(12.8 g/cm^2) were used. The average π^- energy in the targets, $(E_{in} + E_{out})/2$, was ~235 MeV in LiF and ~230 MeV in ^{27}Al and ^{51}V.

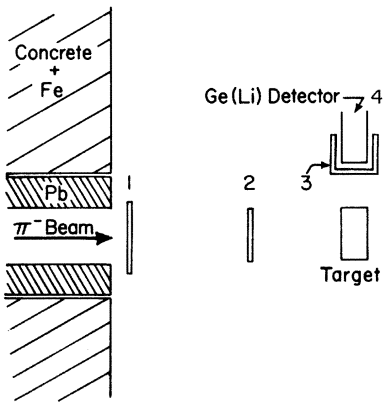

FIG. 1. Experimental geometry. Counters Nos. 1, 2, and 3 are plastic scintillators. Valid events consisted of $12\bar{3}4$ coincidences.

γ rays were detected with a Ge(Li) detector located at 90° with respect to the incident beam. A scintillation cup (No. 3) surrounded the Ge(Li) detector in order to veto charged particle events. γ rays coincident with the beam telescope and anticoincident with counter No. 3 were energy-analyzed and stored in the first half of a gain-stabilized 4096-channel analyzer. The overall resolution of the system was ~5 keV at 1 MeV; the energy range was from ~0.3 to ~6.5 MeV for the ^{19}F and ^{27}Al runs and from ~0.2 to ~6.5 MeV for the ^{51}V runs. The detector dead time was kept low by gating out the prompt burst at the start of each beam pulse and by stretching the remainder of the beam pulse. This procedure resulted in an effective duty factor of at least 60%.

Background and random contributions to the spectra were identified by recording in the second half of the analyzer a spectrum consisting of events in the Ge(Li) detector that were delayed by ~50 nsec relative to true coincidence events. For each target run, these delayed-coincidence spectra were normalized and subtracted from the coincident spectra to eliminate random and background peaks. Prompt background due to secondary interactions and to pion interactions outside the target was not eliminated by this procedure.

Energy calibration was accomplished using standard sources. The relative photopeak efficiency of the Ge(Li) detector was determined by recording a ^{56}Co γ ray spectrum with approximately 20 peaks of known relative intensity. The resultant relative efficiency curve was normalized to an absolute efficiency curve using calibrated source spectra taken at the target position.

III. DATA ANALYSIS

Portions of the spectra from each of the three targets are shown in Figs. 2–4. The peaks were fitted to a Gaussian line shape using a least-squares computer program. Peaks were identified with the decay of particular residual nucleus levels using published excitation energy, lifetime, and branching ratio results.[22-24] Assignments were made only when the measured energy value differed by less than 3 keV from the accepted one.

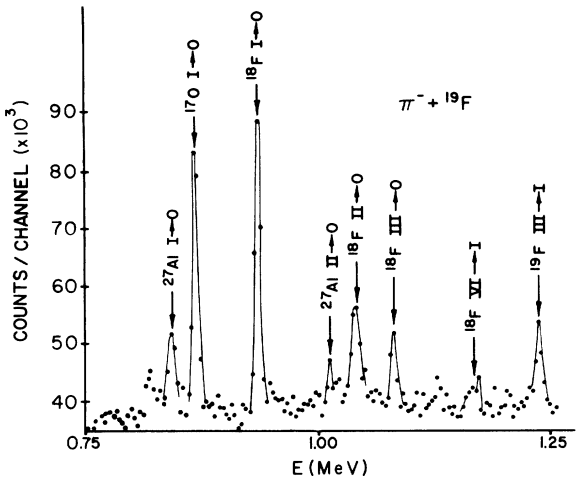

FIG. 2. Portion of the prompt γ ray spectrum from the interaction of 235 MeV π^- with $Li^{19}F$. Arrows indicate nominal photopeak positions. The ^{27}Al peaks are due to background (see text).

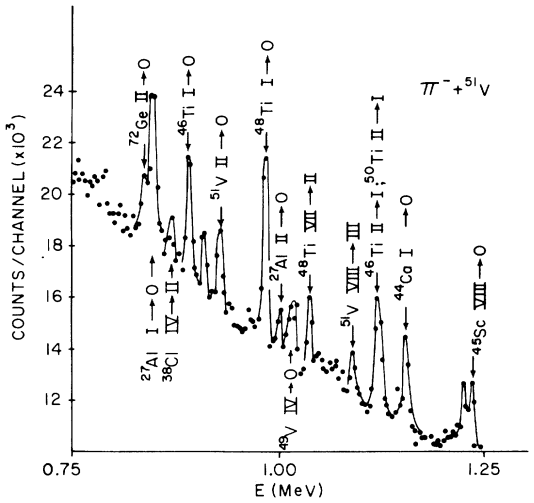

FIG. 4. Portion of the prompt γ ray spectrum from the interaction of 230 MeV π^- with ^{51}V. Arrows indicate nominal photopeak positions. The ^{27}Al peaks are due to background (see text).

The cross section for excitation of each state was computed in the conventional manner from the area of the peak, the absolute detector efficiency corrected for γ ray absorption in the target, the decay branching ratios, the target parameters, and the number of incident pions. It was assumed that the γ rays were emitted isotropically. For states that decayed by several γ branches, the cross sections calculated for the different decay branches had to be compatible before the result was accepted. The cross sections calculated in this manner are shown in Tables I–III for the ^{19}F, ^{27}Al, and ^{51}V targets, respectively, and are labeled α. These are cross sections for excitation of each state, whether the population occurs initially or as a result of the γ decay of higher excited states.

It would be desirable to correct these cross sections for γ feeding from all bound states; but the possibility of γ feeding from many bound states, each excited too weakly to be detected in our experiment, precludes a unique determination for most residual nuclei. We subtracted, therefore, the γ feeding from those higher energy levels for which a cross section could be determined. The results are labeled σ in Tables I–III. The possibility that γ feeding from many other weakly excited bound states may have significantly augmented the values of σ will be examined in Sec. IV.

All spectra were contaminated to approximately the same extent by peaks resulting from π^- and secondary nucleon reactions in the aluminum cylinder surrounding the Ge(Li) detector. By comparing the resulting contamination in the LiF and ^{51}V spectra (see, e.g., Figs. 2 and 4), the probable contamination to the ^{27}Al spectra (see, e.g., Fig. 3) was estimated to be 10%, and these cross sections were reduced accordingly.

Since pion-nuclear interactions were studied by indirect means in the present work, contamination by secondary neutrons to the observed inelastic and single charge exchange cross sections may be significant. An analysis of five peaks in the ^{51}V spectra which result from neutron inelastic scattering on Ge in the Ge(Li) detector indicates that the maximum neutron energy was ~3 MeV, which is less than the minimum Q value for nucleon removal. In a recent 200 MeV π^- run in which a 10 cm diam ^{51}V target was varied in thickness from 1 to 5 g/cm^2, it was found that the inelastic cross

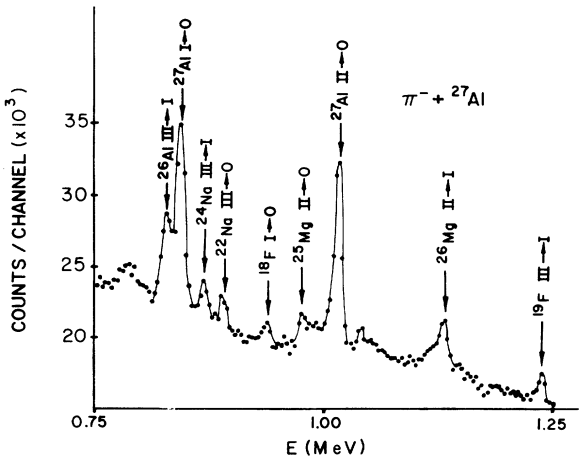

FIG. 3. Portion of the prompt γ ray spectrum from the interaction of 230 MeV π^- with ^{27}Al. Arrows indicate nominal photopeak positions.

TABLE I. Cross sections for 235 MeV π^- interactions with $Li^{19}F$.

Residual nucleus	E_{ex} (MeV)	J^π	Transition detected	α [a] (mb)	σ [b] (mb)	ΔP (MeV/c)
$^{19}_{9}F$	0.110	$\frac{1}{2}^-$	c			
	0.197	$\frac{5}{2}^+$	c			
	1.346	$\frac{5}{2}^-$	III→I	8.0± 1.4 [d]	8.0± 1.4 [d]	
	1.459	$\frac{3}{2}^-$	IV→0	<5.5		
	1.554	$\frac{3}{2}^+$	V→II	18.4± 2.6 [d]	18.4± 2.6 [d]	110
	2.780	$\frac{9}{2}^+$	VI→II	1.8± 1.1 [d]	1.8± 1.1 [d]	
$^{19}_{8}O$	0.096	$\frac{3}{2}^+$	c			
	1.472	$\frac{1}{2}^+$	c			
	2.371	$(\frac{9}{2})$	III→0	<1.4		
$^{18}_{9}F$	0.937	3^+	I→0	21.7± 3.5	18.9± 3.3	
	1.042	0^+	II→0	11.6± 2.0	9.0± 1.9	70
	1.081	0^-	III→0	4.6± 1.0	2.1± 1.2	
	1.122	5^+	c			
	1.701	1^+	V→II	4.1± 1.2	4.0± 1.2	
	2.101	2^-	VI→I	7.7± 2.9	7.7± 2.9	
	2.524	2^+	VII→0	1.6± 0.4	1.6± 0.4	
$^{18}_{8}O$	1.982	2^+	I→0	23.7± 4.1	11.1± 3.3	
	3.553	4^+	II→I	1.9± 0.6	1.9± 0.6	
	3.632	0^+	III→I	8.3± 1.6	3.2± 2.2	70
	3.919	2^+	IV→I	<1.2		
	4.449	1^-	V→I	7.5± 3.0	7.5± 3.0	
$^{17}_{9}F$	0.495	$\frac{1}{2}^+$	I→0	4.0± 1.6	4.0± 1.6	
$^{17}_{8}O$	0.871	$\frac{1}{2}^+$	I→0	20.1± 3.0	20.1± 3.0	
	3.055	$\frac{1}{2}^-$	I→0	<6.2		
$^{17}_{7}N$	1.371	$\leqslant\frac{3}{2}$	I→0	<3.7		
$^{16}_{8}O$	6.131	3^-	II→0	8.5± 2.8	8.5± 2.8	
$^{16}_{7}N$	0.121	0^-	c			
$^{15}_{8}O$	5.181	$\frac{1}{2}^+$	c			
	5.242	$\frac{5}{2}^+$	II→0	1.1± 0.4	1.1± 0.4	
$^{15}_{7}N$	5.271	$\frac{5}{2}^+$	I→0	7.8± 2.3	7.8± 2.3	
	5.299	$\frac{1}{2}^+$	c			
$^{15}_{6}C$	0.747	$\frac{5}{2}^+$	I→0	1.7± 0.6	1.7± 0.6	
$^{14}_{7}N$	2.313	0^+	I→0	8.7± 2.6 [e]	8.2± 2.5 [e]	90
	3.945	1^+	II→I	<5.2		
	4.913	$(0,1)^-$	c			
	5.106	2^-	IV→0	2.1± 0.9	1.2± 1.1	
	5.691	1^-	c			
	5.833	3^-	VI→IV	1.1± 0.5	1.1± 0.5	
^{14}C	6.093	1^-	c			
	6.589	0^+	c			
	6.728	3^-	III→0	1.5± 0.4	1.5± 0.4	
$^{13}_{6}C$	3.086	$\frac{1}{2}^+$	c			
	3.684	$\frac{3}{2}^-$	II→0	1.8± 0.7	0.8± 0.8	
	3.854	$\frac{5}{2}^+$	III→0	2.7± 0.9	2.7± 0.9	
$^{12}_{6}C$	4.439	2^+	I→0	39.8±16.6 [f]	39.8±16.6 [f]	160
$^{12}_{5}B$	0.953	2^+	c			

TABLE I (*Continued*)

Residual nucleus	E_{ex} (MeV)	J^π	Transition detected	α [a] (mb)	σ [b] (mb)	ΔP (MeV/c)
	1.674	2^-	II→0	<2.9		
$^{11}_{6}$C	1.995	$\frac{1}{2}^-$	I→0	<1.9		
$^{11}_{5}$B	2.124	$\frac{1}{2}^-$	I→0	<8.1		
$^{10}_{5}$B	0.717	1^+	I→0	9.0± 1.6[f]	9.0±1.6[f]	
	1.740	0^+	c			
$^{7}_{3}$Li	0.478	$\frac{1}{2}^-$	I→0	16.7± 3.9[g]	16.7± 3.9[g]	120

[a] α is the cross section for production of a particular state by direct excitation and/or by γ feeding from higher states.

[b] σ is the result of correcting α for γ feeding from higher states known to be excited.

[c] Cross section or upper limit could not be determined.

[d] Cross section should be considered an upper limit due to possible contributions from secondary neutrons.

[e] Cross section should be considered an upper limit due to possible contribution from an overlapping transition.

[f] Cross section may be contaminated up to 25% by π^- interactions on ^{12}C in the scintillation counters.

[g] Cross section assumed to be due to inelastic scattering of π^- and/or secondary neutrons on ^{7}Li in the LiF target.

TABLE II. Cross sections for 230 MeV π^- interaction with ^{27}Al.

Residual nucleus	E_{ex} (MeV)	J^π	Transition detected	α [a] (mb)	σ [b] (mb)	ΔP (MeV/c)
$^{27}_{13}$Al	0.844	$\frac{1}{2}^+$	I→0	25.0±3.9[c]	24.1±3.8[c]	
	1.014	$\frac{3}{2}^+$	II→0	29.9±4.8[c]	22.9±4.0[c]	
	2.211	$\frac{7}{2}^+$	III→0	26.7±4.9[c]	21.9±4.4[c]	110
	2.734	$\frac{5}{2}^+$	IV→II	9.1±1.7[c]	9.1±1.7[c]	80
	2.981	$\frac{3}{2}^+$	V→0	3.8±1.5[c]	3.8±1.5[c]	70
	3.004	$\frac{9}{2}^+$	VI→0	16.3±3.6[c]	15.5±3.5[c]	100
	3.678	$\frac{1}{2}^+$	VII→I	<4.0		
	3.956	$(\frac{3}{2},\frac{5}{2})^+$	VIII→0	<3.6		
	4.054	$(\frac{1}{2},\frac{3}{2})^-$	IX→I	<2.8		
	4.409	$\frac{5}{2}^+$	X→0	<4.0		
	4.510	$\frac{11}{2}^+$	XI→III	3.5±1.3[c]	3.5±1.3[c]	80
$^{27}_{12}$Mg	0.985	$\frac{3}{2}^+$	d			
	1.698	$\frac{5}{2}^+$	II→0	1.7±0.4[c]	1.7±0.4[c]	
$^{26}_{13}$Al	0.228	0^+	d			
	0.417	3^+	II→0	10.1±1.9	5.2±1.9	
	1.058	1^+	III→II	19.4±3.2	19.4±3.2	
	1.759	2^+	IV→II	<2.4		
	1.851	1^+	d			
	2.069	4^+	VI→II	5.1±2.1	5.1±2.1	
	2.070	2^+	VII→III	<5.9		
	2.072	1^+	VIII→I	<1.7		
	2.365	3^+	IX→II	<3.3		
	2.545	3^+	X→VI	4.3±1.0	4.3±1.0	
$^{26}_{12}$Mg	1.809	2^+	I→0	43.9±7.9	33.5±6.7	80
	2.938	2^+	II→I	11.5±2.1	11.5±2.1	110

TABLE II (*Continued*)

Residual nucleus	E_{ex} (MeV)	J^{π}	Transition detected	α [a] (mb)	σ [b] (mb)	ΔP (MeV/c)
$^{25}_{13}$Al	0.452	$\frac{1}{2}^+$	I→0	<1.6		
	0.945	$\frac{3}{2}^+$	II→I	<1.5		
$^{25}_{12}$Mg	0.585	$\frac{1}{2}^+$	I→0	6.1±1.1	3.0±0.9	
	0.975	$\frac{3}{2}^+$	II→I	6.2±1.3	6.2±1.3	
	1.612	$\frac{7}{2}^+$	III→0	13.9±3.2 [e]	5.4±3.3 [e]	130
	1.965	$\frac{5}{2}^+$	d			
	2.564	$\frac{1}{2}^+$	d			
	2.736	$\frac{7}{2}^+$	VI→II	<2.3		
	2.801	$\frac{3}{2}^+$	VII→0	<6.2		
	3.405	$\frac{9}{2}^+$	VIII→III	10.2±3.1	10.2±3.1	
$^{25}_{11}$Na	0.090	$(\frac{3}{2}, \frac{5}{2})^+$	d			
	1.069	$\frac{1}{2}^+$	II→I	<3.7		
$^{24}_{12}$Mg	1.369	2^+	I→0	33.5±5.3	28.8±4.8	
	4.123	4^+	II→I	4.7±1.3	4.7±1.3	90
$^{24}_{11}$Na	0.472	1^+	d			
	0.563	2^+	d			
	1.341		III→I	3.9±0.8 [e]	3.9±0.8 [e]	
	1.345	3	IV→0	<5.0		
	1.347	1^+	V→I	<4.2		
$^{24}_{10}$Ne	1.981	2^+	d			
	3.867	2^+	II→I	<6.0		
$^{23}_{12}$Mg	0.451	$\frac{5}{2}^+$	I→0	<2.1		
$^{23}_{11}$Na	0.440	$\frac{5}{2}^+$	I→0	20.7±3.8	20.7±3.8	
	2.076	$\frac{7}{2}^+$	II→I	<8.3		
$^{23}_{10}$Ne	1.016	$\frac{1}{2}^+$	d			
	1.703	$\frac{7}{2}$	II→0	<2.2		
$^{22}_{12}$Mg	1.247	2^+	I→0	<1.1		
$^{22}_{11}$Na	0.583	1^+	d			
	0.657	0^+	d			
	0.891	4^+	III→0	3.6±1.2	3.6±1.2	
$^{22}_{10}$Ne	1.275	2^+	I→0	15.9±2.6	15.9±2.6	
	3.356	4^+	II→I	<3.3		
$^{21}_{11}$Na	0.332	$\frac{5}{2}^+$	I→0	0.7±0.3	0.7±0.3	
$^{21}_{10}$Ne	0.351	$\frac{5}{2}^+$	I→0	13.2±2.5	13.2±2.5	
	1.746	$\frac{7}{2}^+$	d			
$^{21}_{9}$F	0.280	$\frac{1}{2}^+$	d			
	1.101	$(\frac{1}{2}, \frac{3}{2})^-$	d			
	1.730		III→0	<4.5		
$^{20}_{10}$Ne	1.634	2^+	I→0	14.7±2.6	11.7±2.4	
	4.247	4^+	d			
	4.968	2^-	III→I	3.0±1.0	3.0±1.0	
$^{20}_{9}$F	0.656	3^+	I→0	3.3±0.8	3.3±0.8	120
	0.823	$4^+, 2^+$	d			
$^{19}_{10}$Ne	0.238	$\frac{5}{2}^+$	d			
	0.275	$\frac{1}{2}^-$	d			
	1.508	$\frac{5}{2}^-$	III→II	<2.1		

TABLE II (*Continued*)

Residual nucleus	E_{ex} (MeV)	J^π	Transition detected	α [a] (mb)	σ [b] (mb)	ΔP (MeV/c)
$^{19}_{9}$F	0.110	$\frac{1}{2}^-$	d			
	0.197	$\frac{5}{2}^+$	d			
	1.346	$\frac{5}{2}^-$	III→I	5.4±1.0	5.4±1.0	
	1.458	$\frac{3}{2}^-$	d			
$^{19}_{8}$O	0.096	$\frac{3}{2}^+$	d			
	1.472	$\frac{1}{2}^+$	d			
$^{18}_{10}$Ne	1.887	2^+	I→0	<3.3		
	3.376	4^+	II→I	2.1±0.5	2.1±0.5	
$^{18}_{9}$F	0.937	3^+	I→0	3.9±0.8	3.9±0.8	
	1.042	0^+	d			
$^{18}_{8}$O	1.982	2^+	d			
	3.553	0^+	II→I	<1.5		
$^{17}_{9}$F	0.495	$\frac{1}{2}^+$	I→0	<0.6		
$^{17}_{8}$O	0.871	$\frac{1}{2}^+$	I→0	<4.5		
	3.055	$\frac{1}{2}^-$	II→I	<3.6		
$^{17}_{7}$N	1.371	$\leq\frac{3}{2}$	d			
$^{16}_{8}$O	6.131	3^-	II→0	7.3±2.3	7.3±2.3	
$^{15}_{8}$O	5.242	$\frac{5}{2}^+$	II→0	<0.5		
$^{15}_{7}$N	5.271	$\frac{5}{2}^+$	I→0	2.0±0.6	2.0±0.6	

[a] α is the cross section for production of a particular state by direct excitation and/or by feeding from higher states.

[b] σ is the result of correcting α for γ feeding from higher states known to be excited.

[c] Cross section should be considered an upper limit due to possible contributions from secondary neutrons.

[d] Cross section or upper limit could not be determined.

[e] Cross section should be considered an upper limit due to possible contributions from an overlapping transition.

TABLE III. Cross sections for 230 MeV π^- interactions with ^{51}V.

Residual nucleus	E_{ex} (MeV)	J^π	Transition detected	α [a] (mb)	σ [b] (mb)
$^{51}_{23}$V	.320	$\frac{5}{2}^-$	I→0	137±30 [c]	105±25 [c]
	.929	$\frac{3}{2}^-$	II→0	33±5 [c]	33±5 [c]
	1.609	$\frac{11}{2}^-$	III→0	82±15 [c]	67±12 [c]
	1.813	$\frac{9}{2}^-$	IV→0	58±12 [c]	58±12 [c]
	2.409	$\frac{3}{2}^-$	V→I	17±3 [c]	17±3 [c]
	2.699	$\frac{15}{2}^-$	VIII→III	16±4 [c]	16±4 [c]
$^{51}_{22}$Ti	1.160	$\frac{1}{2}^-$	I→0	<2	
	1.429	$\frac{7}{2}^-$	II→0	<4	
	1.559	$\frac{5}{2}^-, \frac{7}{2}^-$	III→0	<10	
	2.136	$\frac{5}{2}^-, \frac{7}{2}^-$	IV→0	<7	

TABLE III (*Continued*)

Residual nucleus	E_{ex} (MeV)	J^{π}	Transition detected	α [a] (mb)	σ [b] (mb)
$^{50}_{23}$V	.226	5^+	I→0	126±33	116±31
	.320	4^+	d		
	.355	$(3)^+$	d		
	.388	2^+	d		
	.836	(5^+)	d		
	.911	(4^+)	VI→I	7±3	7±3
	1.301	(2^+)	VII→IV	<7	
	1.331	1^+	VIII→I	3±1	3±1
$^{50}_{22}$Ti	1.554	2^+	I→0	31±6	<14
	2.677	4^+	II→I	76±13 [e]	76±13 [e]
	3.201	$(6)^+$	III→II	<7	
$^{49}_{23}$V	0.090	$\frac{5}{2}^-$	d		
	0.153	$\frac{3}{2}^-$	d		
	0.748	$\frac{3}{2}$	III→I	4±2	4±2
	1.022		IV→0	14±3	14±3
$^{49}_{22}$Ti	1.382	$\frac{3}{2}^-$	I→0	9±2	9±2
	1.542	$\frac{5}{2}^+-\frac{19}{2}$	II→0	27±6	27±6
	1.585	$\frac{3}{2}, \frac{5}{2}$	III→0	13±3	13±3
$^{48}_{22}$Ti	0.982	2^+	I→0	73±12	<18
	2.295	4^+	II→I	64±14	30±8
	2.421	(2^+)	III→I	10±3	10±3
	3.332	6^+	VIII→II	34±6 [f]	34±6 [f]
$^{48}_{21}$Sc	0.131	(5^+)	d		
	0.252	(4^+)	d		
	0.622	(3^+)	III→II	8±3	<5
	1.143	$(1, 2^+)$	d		
	1.402	(2^-)	V→III	9±3	9±3
$^{47}_{22}$Ti	0.159	$(\frac{7}{2}^-)$	d		
	1.247	$(\frac{9}{2}^-)$	II→0	7±2	7±2
	1.549	$(\frac{3}{2}^-)$	IV→I	<6	
$^{47}_{21}$Sc	0.767	$\frac{3}{2}^+$	I→0	<2	
	0.808	$\frac{3}{2}^-$	II→0	7±2	7±2
$^{46}_{22}$Ti	0.889	2^+	I→0	48±9 [f]	<14
	2.010	4^+	II→I	e	e
$^{46}_{20}$Ca	1.347	2^+	I→0	10±5	10±5
$^{45}_{21}$Sc	0.012	$\frac{3}{2}^+$	d		
	0.376	$\frac{3}{2}^-$	II→I	<3	
	0.543	$\frac{5}{2}^+$	III→0	7±2	7±2
	1.237	$(\frac{5}{2}^--\frac{11}{2}^-)$	VIII→0	30±6	30±6
$^{44}_{20}$Ca	1.157	2^+	I→0	38±7	38±7
$^{42}_{20}$Ca	1.524	2^+	I→0	26±5	26±5
$^{40}_{20}$Ca	3.737	3^-	II→0	<8	

TABLE III *(Continued)*

Residual nucleus	E (MeV)	J^π	Transition detected	α [a] (mb)	σ [b] (mb)
$^{38}_{17}$Cl	0.671	5^-	I→0	7±2	7±2
	0.755	3^-	II→0	<10	
	1.309	4^-	d		
	1.617	3^-	IV→II	5±2	5±2

[a] α is the cross section for production of a particular state by direct excitation and/or by γ feeding from higher states.

[b] σ is the cross section α corrected for γ feeding from states known to be excited.

[c] Cross section should be considered an upper limit due to possible contributions from secondary neutrons.

[d] Cross section or upper limit could not be determined.

[e] Measured strength shared between ^{50}Ti II→I and ^{46}Ti II→I.

[f] Cross section should be considered an upper limit due to possible contributions from an overlapping transition.

section increased approximately linearly with target thickness. The extrapolation of these data to the present results indicates that approximately 75% of the observed ^{51}V cross section is due to these secondary neutrons. The inelastic cross sections for ^{19}F and ^{27}Al would not necessarily include the same secondary neutron contamination, but such contamination is likely to be large. The data of cross section vs target thickness indicated that there was no neutron contamination to the single and multiple nucleon removal cross sections.

The errors shown in Table I–III were calculated from estimated uncertainties in all factors affecting the cross sections. Major contributions were the statistical uncertainty resulting from the least-squares fitting procedure, the energy-dependent error in the relative efficiency, and the error in the absolute efficiency normalization which was 15%. The relative error in comparing cross sections for the same target is smaller than the total error and is obtained by subtracting (in quadrature) the absolute error from the total error.

γ ray peaks resulting from the decay of short-lived ($\leq$1 psec) states showed Doppler broadening due to the recoil momentum of the product nucleus. Nuclear recoil momenta were calculated by unfolding the intrinsic line widths from the broadened spectrum peaks and evaluating the expression for $S(\tau_m)$, the slowing down of the recoil nucleus in the target material, with a computer program based on the work of Ref. 25. Results for levels showing measurable broadening are listed in the last column of Tables I–III. Since the errors in the Doppler broadening are quite large, an analysis using the unfolding technique of Lewis[26] is unjustified.

The reported upper-limit estimates for the unobserved transitions (Tables I–III) were based on the following considerations. Expected peak widths were estimated by assuming that the recoil momenta obtained for observed peaks were typical and by correcting for slowing down of the residual nucleus using the reported lifetimes τ_m for the initial state. The estimated Doppler-broadened peak width was then folded into the system intrinsic width to obtain a maximum linewidth. Using this result and the known branching ratios, an upper limit of the amplitude for these weak levels was estimated either by inspection or by using a least-squares fitting procedure with width and center channel fixed. From this value, the corresponding cross section was computed in the usual manner.

IV. RESULTS AND DISCUSSION

The results for π^- interactions with ^{19}F, ^{27}Al, and ^{51}V presented in Tables I, II, and III, respectively, will first be considered separately for each target with emphasis on individual features (Secs. IV A–IV C). In Sec. IV D, systematic features of the results will be discussed and compared with the predictions of several intranuclear cascade/evaporation (INC/E) calculations. Single nucleon removal ratios will be discussed in a separate paper.

A. ^{19}F target results

A striking feature of the results shown in Table I is the size of some of the cross sections for removal of a large number of nucleons. Two of these cross sections, those for production of ^{10}B and ^{12}C, may have been augmented by π^- interactions in the plastic scintillation detectors. However, this contamination was estimated to be no higher

than 25% by comparing the ^{19}F spectrum with the ^{27}Al and ^{51}V spectra where the ^{10}B and ^{12}C transitions were very weak. The broad ^{12}C, 4.439 MeV peak overlaps the position of a possible peak due to the II → 0, 4.444 MeV transition in ^{11}B which would also be Doppler-broadened; but because of the low upper limit for the I → 0 transition in ^{11}B (Table III), the observed peak was assumed to be due primarily to the I → 0, 4.439 MeV transition in ^{12}C. The ^{7}Li cross section reported in Table III is presumed to be due entirely to π^- inelastic scattering on ^{7}Li (92.6% isotopic abundance) in the LiF target.

The observed cross section for removal of an equivalent α particle (resulting in ^{15}N) is also relatively large, but the equivalent t removal cross section resulting in ^{16}O is even larger; equivalent $t+\alpha$ removal (resulting in ^{12}C) has the largest multiple nucleon removal cross section observed for this target, even after the possible 25% contamination due to π^- interactions in the plastic scintillators is taken into account. The reported ^{15}N, 5.271 MeV level cross section is probably indicative of the entire ^{15}N cross section because of the strong feeding of this level from higher levels.

The next highest cross section for multiple nucleon removal from ^{19}F is that for $n+p$ (or equivalent d) removal resulting in ^{17}O. Equivalent ^{3}He removal cross sections could not be determined for the ^{19}F target, because states in ^{16}N could not be observed; for equivalent ^{3}He$+\alpha$ removal resulting in ^{12}B, a low upper limit was determined for the II → 0 transition.

The single nucleon removal cross sections are compared with experimental single nucleon transfer spectroscopic factors[28] in Table IV. In interpreting this comparison, the possible effect of γ feeding from states with a large spectroscopic factor and a relatively high upper limit must be considered. In ^{18}F, e.g., the 3.060 and 3.135 MeV levels branch strongly to the first two excited states. If the 3.060 and 3.135 MeV states were excited to as much as half of their reported upper limits, the subsequent γ feeding would increase the cross sections for the first two states relative to the third excited state. The reported cross sections for the 1.701 and 2.101 MeV states in ^{18}F which have low spectroscopic factors cannot be explained by γ feeding from higher-energy states. In ^{18}O, feeding from states with high spectroscopic factors could explain the reported 3.632 and 4.449 MeV cross sections. A consideration of possible feeding contributions may thus account for some but not all of the differences between relative values of spectroscopic factors and measured cross sections.

The observed summed single neutron removal cross section, 43 ± 11 mb, can be compared with an activation determination of the ^{19}F(π^-,π^-n)^{18}F cross section[11] at 220 MeV, 25 ± 5 mb. Since ground state formation without prior excited state formation and γ decays from some states are missed in the present work, one would expect the summed cross section to be less than or at most equal to the activation result. A more recent activation determination[27] of that cross section resulted in a value of 45 ± 3 mb at 235 MeV, in better agreement with the present prompt γ ray work.

The sum of all measured and corrected $\pi^- + ^{19}$F cross sections σ is 174 mb (not including inelastic scattering, upper limits, and the ^{7}Li cross section). The INC/E calculation described in Sec. IV D results in a geometric cross section of 905 mb and a total single and multiple nucleon removal cross section of 516 mb. The measured cross sections thus represent approximately 34% of this total, which is in reasonable agreement with the calculated result since in a prompt γ ray experi-

TABLE IV. Comparison of 235 MeV π^- induced single nucleon removal cross sections on ^{19}F with direct reaction spectroscopic factors.

Residual nucleus	E_{ex} (MeV)	J^π	220 MeV π^- σ[a] (mb)	C^2S
		^{19}F(p,d)^{18}F[b]		
^{18}F	0	1$^+$	c	0.62
	0.937	3$^+$	18.9 ± 3.3	1.2
	1.042	0$^+$	9.0 ± 1.9	0.31
	1.081	0$^-$	2.1 ± 1.2	0.41
	1.122	5$^+$	c	
	1.701	1$^+$	4.0 ± 1.2	0.06
	2.101	2$^-$	7.7 ± 2.9	<0.13
	2.524	2$^+$	1.6 ± 0.4	≈0.13
	3.060	2$^+$	<6.4	0.53
	3.135	1$^-$	<8.1	0.88
		^{19}F(d,^{3}He)^{18}O[b]		
^{18}O	0	0$^+$	c	0.38
	1.982	2$^+$	11.1 ± 3.3	0.53
	3.553	4$^+$	1.9 ± 0.6	
	3.632	0$^+$	3.2 ± 2.2	0.05 ± 0.02
	3.919	2$^+$	<1.2	0.02 ± 0.01
	4.449	1$^-$	7.5 ± 3.0	1.31
	5.690	3$^-$	<2.8	
	5.250	2$^+$	<5.0	0.32 ± 0.1
	5.329	0$^+$	<4.5	0.15 ± 0.06
	6.191	1$^-$	<6.4	0.70[d]
	6.86	0$^-$	<3.8	1.03
	7.62	1$^-$	c	0.42[d]

[a] This work; corrected for γ feeding from higher states known to be excited (see Table I).

[b] See Ref. 28.

[c] Cross section or upper limit could not be determined.

[d] Doublet not resolved.

ment one expects to miss a fraction of the total cross section due to direct ground state formation, decay of states too weakly excited to be detected, and decays resulting in γ ray energies outside the range of the apparatus.

The INC/E calculations (Sec. IV D) predict that π^- absorption in flight is likely to occur in as much as $\frac{1}{3}$ of all π^- induced reactions at 200 MeV. Because the π^- rest energy is available in these reactions, they are likely to produce a greater mass change, ΔA, than the nonabsorptive interactions. In Table V, the measured γ ray yields for stopped π^- absorption[29] are compared with the present cross sections. Since nonabsorptive reactions will predominate for small ΔA, it is reasonable to compare those cross sections for ΔA greater than ~2. We find quantitatively similar excitation for states of ^{16}O, ^{15}N, ^{14}N, ^{14}C, and ^{13}C. There is disagreement for the first excited states of ^{14}N, ^{12}C, and ^{10}B. But the ^{14}N cross section is doubtful because the peak is overlapped by several transitions, and the ^{12}C and ^{10}B cross sections may be contaminated up to 25% by π^- reactions in the scintillation counters. The additional kinetic energy available in the present π^- work is likely to result in more multiple nucleon removal than in the stopped π^- experiment, if the available energy is shared among the nuclear constituents. Hence some differences in the removed mass spectra are expected for the two experiments, even if absorption in flight were dominant in the 235 MeV π^- experiment.

B. ^{27}Al target results

In the $\pi^- + {}^{27}$Al interaction, a considerable variety of residual nuclei was detected (Table II). Removal of one, two, and three equivalent α particles resulting in ^{23}Na, ^{19}F, and ^{15}N, respectively, is conspicuous; but equivalent t, $t+\alpha$, and $t+2\alpha$ removal resulting in ^{24}Mg, ^{20}Ne, and ^{16}O, respectively, is consistently stronger than the corresponding α or multiple α removal, while equivalent ^{3}He and ^{3}He$+\alpha$ removal is considerably weaker. The possibility of π^- absorption on a cluster within the nucleus resulting in the removal of the cluster and leaving the residual nucleus in a high spin state from which subsequent evaporation of α particles is preferred will be discussed in Sec. IV D.

Equivalent d (or $n+p$) removal is second in strength only to equivalent t removal among the multiple nucleon removals, but weaker than single nucleon removal. The single nucleon removal cross sections are compared with direct reaction spectroscopic factors in Table VI. Consideration of γ feeding from higher energy states with large spectroscopic factors could not account for the relative cross sections of the second and third excited states of ^{26}Al. The low upper limit for the 4.332 MeV level in ^{26}Mg which has a large spectro-

TABLE V. Comparison of 235 MeV $\pi^- + {}^{19}$F cross sections with yields from stopped $\pi^- + {}^{19}$F.

Residual nucleus	E_{ex} (MeV)	220 MeV π^- α [a] (mb)	Stopped π^- yield $N\gamma/N_\pi$ [b] (%)
^{18}O	1.982	23.7 ± 4.1	1.4
^{17}O	0.871	20.1 ± 3.0	1.3
^{16}O	6.131	8.5 ± 2.8	1.9
^{15}N	5.271	7.8 ± 2.3	2.3
^{14}C	6.728	1.8 ± 0.7	0.51
^{13}C	3.684	2.7 ± 0.9	0.94
^{12}C	4.44	39.8 ± 16.6 [c]	1.4

[a] This work; α is the cross section for production of a particular state by direct excitation and/or by γ feeding from higher states (see Table I).

[b] See Ref. 29.

[c] Cross section may be contaminated up to 25% by π^- interactions on ^{12}C in the scintillation counters.

TABLE VI. Comparison of 230 MeV π^- induced single nucleon removal cross sections on ^{27}Al with direct reaction spectroscopic factors.

Residual nucleus	E_{ex} (MeV)	J^π	220 MeV π^- σ [a] (mb)	C^2S
	^{27}Al$(p,d)^{26}$Al [b]			
^{26}Al	0	5$^+$	c	0.57
	0.228	0$^+$	c	0.10
	0.417	3$^+$	5.2 ± 1.9	0.14
	1.058	1$^+$	19.4 ± 3.2	0.16
	1.759	2$^+$	<2.4	0.013
	1.851	1$^+$	c	0.006
	2.069	4$^+$	5.1 ± 2.1	
	2.070	2$^+$		
	2.072	1$^+$		
	2.365	3$^+$		
	2.545	3$^+$	4.3 ± 1.0	0.30
	^{27}Al$(d,{}^3$He$)^{26}$Mg [b]			
^{26}Mg	0	0$^+$	c	0.26
	1.809	2$^+$	33.5 ± 6.7	0.85
	2.938	2$^+$	11.5 ± 2.1	0.24
	4.332	2	<6.0	2.05
	5.474	4$^+$	c	0.25
	6.127	2$^+$	c	0.056
	7.25		c	0.34
	7.86		c	1.1

[a] This work; corrected for γ feeding from higher states known to be excited (see Table II).

[b] See Ref. 23.

[c] Cross section or upper limit could not be determined.

scopic factor is another clear difference between the relative values of spectroscopic factors and measured cross sections.

The cross sections observed in this work are compared in Table VII with the results of a similar prompt γ ray experiment, in which 70 MeV π^- interacted with ^{27}Al.[5] In that work, no γ feeding corrections were made; hence our uncorrected values, α, rather than the σ values are compared with the results of the 70 MeV work. Generally, residual levels excited strongly in the present work also show up prominently in the 70 MeV experiment. Furthermore, the 230 MeV cross sections for inelastic scattering and single nucleon removal are, on the average, almost 3 times as large as the corresponding cross sections in the 70 MeV experiment, in general agreement with the energy dependence of the (3,3) resonance. Most of the cross sections for multiple nucleon removal are nearly equal at 70 and 230 MeV, which would suggest a lack of resonance behavior for these reaction channels.

The sum of all corrected $\pi^- + {}^{27}$Al cross sections σ is 234 mb (not including inelastic scattering and upper limits). The INC/E calculation resulted in a geometric cross section of 1028 mb and a total single and multiple nucleon removal cross section of 655 mb. The measured cross sections represent, therefore, about 36% of this total.

C. ^{51}V target results

The greater complexity of the energy level and decay schemes of the residual nuclei in the $A = 40$ to 50 region made the interpretation of the $\pi^- + {}^{51}$V results more ambiguous than the interpretation of the lower-mass target results. Equivalent t and $t+\alpha$ removal (leading to ^{48}Ti and ^{44}Ca, respectively) is even more pronounced than for $\pi^- + {}^{27}$Al, while equivalent α removal (leading to ^{47}Sc) is considerably weaker. Multiple neutron removal, such as removal of $2n$, $3n+p$, $4n+p$, $4n+2p$, has markedly increased for ^{51}V, which is probably a reflection of the larger neutron excess of this target.

The single nucleon removal cross sections are compared with direct reaction spectroscopic factors[30,31] in Table VIII. The ^{50}V comparison is generally inconclusive because decays from the II, III, and IV excited states are too low in energy to be seen and almost all states feed the 0.226 MeV level. One would not expect this level to be excited strongly if the reaction were direct because of its low spectroscopic factor. The low excitation of the 0.911 MeV state, which has a high direct reaction spectroscopic factor, may be indicative of a nondirect reaction mechanism. In ^{50}Ti, the I $\rightarrow$ 0 transition was detected but its strength appears to be due largely to feeding from the II $\rightarrow$ I transition. Since this ^{50}Ti transition is overlapped by the II $\rightarrow$ I transition in ^{46}Ti, the amount of feed-

TABLE VII. Comparison of 230 MeV $\pi^- + {}^{27}$Al with 70 MeV $\pi^- + {}^{27}$Al cross sections.

Residual nucleus	E_{ex} (MeV)	220 MeV π^- α[a] (mb)	70 MeV π^- σ[b] (mb)
^{27}Al	0.844	25.0 ± 3.9[c]	10.2 ± 3.1
^{26}Al	0.417	10.1 ± 1.9	3.7 ± 2.3
^{26}Mg	1.809	43.9 ± 7.9	16.2 ± 4.1
^{25}Mg	0.585	6.1 ± 1.1	10.1 ± 2.1
^{24}Mg	1.369	33.5 ± 5.3	18.3 ± 3.5
^{23}Na	0.440	20.7 ± 3.8	21.9 ± 2.4
^{22}Ne	1.275	15.9 ± 2.6	12.8 ± 3.4
^{21}Ne	0.351	13.2 ± 2.5	14.0 ± 3.5
^{18}F	0.937	3.9 ± 8	≤6.3

[a] This work; α is the cross section for production of a particular state by direct excitation and/or by γ feeding from higher states (see Table II).

[b] See Ref. 5; cross section not corrected for γ feeding.

[c] Cross section should be considered an upper limit due to possible contributions from secondary neutrons.

TABLE VIII. Comparison of 230 MeV π^- induced single nucleon removal cross sections on ^{51}V with direct reaction spectroscopic factors.

Residual nucleus	E_{ex} (MeV)	J^π	230 MeV π^- σ[a] (mb)	C^2S
		^{51}V$(d,t)^{50}$V[b]		
^{50}V	0	6$^+$	c	1.6
	0.226	5$^+$	116 ± 31	0.007 ± 0.69
	0.320	4	c	0.007 ± 1.0
	0.355	3$^+$	c	0.58
	0.388	2$^+$	c	0.33
	0.836	5$^+$	c	0.013 ± 1.1
	0.911	4$^+$	7 ± 3	2.7
	1.301	2$^+$	c	0.34
	1.331	1$^+$	3 ± 1	0.25
	1.400	3$^+$	c	0.012
		^{51}V$(d,{}^3\mathrm{He})^{50}$Ti[d]		
^{50}Ti	0	0$^+$	c	0.74
	1.554	2$^+$	<14	0.37
	2.677	4$^+$	76 ± 13[e]	0.75
	3.201	6$^+$	c	1.14

[a] This work; corrected for γ feeding from higher states known to be excited (see Table III).

[b] See Ref. 30.

[c] Cross section or upper limit could not be determined.

[d] See Ref. 31.

[e] Measured strength shared between ^{50}Ti II $\leftarrow$ I and ^{46}Ti II $\rightarrow$ I.

ing cannot be determined. While there is apparent disagreement between the relative values of the measured single nucleon removal cross sections and the corresponding direct reaction spectroscopic factors, the comparison is not conclusive because of the above ambiguities.

The results for ^{46}Ti, ^{48}Ti, and ^{50}Ti indicate that there is very little excitation of the 2^+ first excited state prior to γ feeding, since the observed $I \rightarrow 0$ γ strength can be accounted for by feeding from higher states.

The sum of all corrected $\pi^- + {}^{51}$V cross sections is 489 mb (again not including inelastic scattering and upper limits), compared with an INC/E calculation result of 1313 mb for the geometric cross section and of 917 mb for the total single and multiple nucleon removal cross sections. The measured cross sections represent more than 50% of this total, which is a larger fraction than was found for the lower-A targets. It should be noted that the uncertainty in the absolute normalization of the cross sections is large and also that there are several possible systematic factors which may have increased this percentage in the case of ^{51}V. A larger fraction of the γ rays in the ^{51}V spectra had $E_\gamma < 0.5$ MeV than in the other spectra. For such γ rays, the target absorption correction is larger, and hence the uncertainty from this correction becomes more significant.

D. Intranuclear cascade/evaporation model calculation results

The great variety of residual nuclei which are produced in these π^- interactions with odd-A target nuclei suggests that some form of statistical process is occurring. Codes based on an intranuclear cascade/evaporation (INC/E) model[32,33] have proved to be a valuable tool in the interpretation of such interactions (see, e.g., Refs. 18, 19, and 36). In these calculations, it is assumed that nuclear reactions of medium and high energy particles can be explained in terms of an initial cascade of particle-particle collisions within the nucleus followed by evaporation of nucleons or nucleon clusters. Free particle cross sections are used with Monte Carlo sampling techniques in order to determine the history of each particle involved in the cascade.

Our results will be compared with the results of calculations with the INC/E codes of Bertini[32] and of Harp *et al.*[33] The overall structure of the two codes is similar, but they differ somewhat in detail.[34] In the cascade phase of the calculation, the Bertini code approximates the nuclear density by a dense central core, surrounded by three annular regions with successively decreasing density. The Harp code uses seven annular regions, but comparisons indicate that the effect of this difference is not significant. In addition, the Harp code includes reflection and refraction at the boundaries between the different density regions, an approximation for the effects of nucleon pair correlations, and the production and subsequent interaction of (3,3) isobars. Finally, each program uses a different code for the subsequent evaporation.[35]

The $\pi^- + {}^{19}$F cross sections were calculated for $E_\pi = 220$ MeV with a copy of the Bertini program provided by the author. Due to computer core limitations, only the first part of that program (INC code MECC7) was used. Instead of using the second part (I4C analysis code), an energy spectrum for each residual nucleus produced in the cascade was obtained from the particle history tape produced by MECC7 and was divided into energy bins. Subsequent evaporation was accomplished with a version of the Blann-Plasil evaporation code.[37] The $\pi^- + {}^{27}$Al cross section results for $E_\pi = 200$ MeV were communicated to us by the authors of the codes.[38,39]

Some general observations can be made on the basis of our INC/E analysis of the $\pi^- + {}^{19}$F interaction. According to the results obtained with the Bertini code, no pions emerge in approximately $\frac{1}{3}$ of all π^- interactions, and $\frac{2}{3}$ of all cascades resulting in a mass removal, ΔA, larger than two involve π^- absorption. In evaporation following π^- absorption, there is an even greater mass change because the resulting residual nuclei are left with a higher excitation energy than in nonabsorptive reactions. The role of absorption in flight has been noted in spallation reactions of 65 MeV π^- and π^+ with Cu, where the yield distribution of the residual nuclei was found to be similar to that of 205 MeV proton reactions.[36] These $\pi^\pm$ + Cu reaction results were adequately reproduced by INC/E calculations.

The INC/E codes assume that π^- absorption occurs on two nucleons. Although this is no doubt the dominant process, absorption on larger clusters may also be important. From a stopped π^- experiment on several nuclei from Li to Pb,[17] most of which were even-even, it was concluded that π^- absorption on α clusters may play a significant role.[17,40,41] Kaons have also been expected to be absorbed on α clusters,[42] resulting in high spin states of the residual nucleus. In the subsequent decay of these high spin states, α emission would be favored over nucleon emission. Evidence that such a process may be operative in π^- absorption has been obtained in a study[43] of π^- capture in ^{12}C in which 1.00 ± 0.07 α particles per pion were detected. The π^- interactions with the odd-Z–even-N targets studied in the present work have shown a marked preference for equivalent t and $t + n\alpha$ re-

moval. This could be an indication of absorption on a t cluster followed by evaporation of α particles. Further experimental and theoretical work is clearly needed to determine the extent to which π^- absorption on clusters is likely to occur and whether such absorption should be included in the INC/E codes.

The INC Bertini code further predicts for $\pi^- + {}^{19}F$ at 200 MeV that $\frac{2}{3}$ of all single nucleon removal interactions result from events in which there was just one collision. This corresponds to a one-step quasifree interaction. Both the Bertini and the Harp codes allow only individual nucleon emission in the cascade stage but allow α emission in the evaporation stage. The evaporated α particle cross section amounts to at least 85 mb in the $\pi^- + {}^{19}F$ calculation (Bertini and Blann) and approximately 210 mb in the $\pi^- + {}^{27}Al$ calculation (Bertini).

A comparison between the present experimental results and the calculated results is complicated by the complexity of the γ decay schemes of the residual nuclei, by the limitations of the prompt γ ray detection method, and by the variation in the fraction of transitions missed from one residual nucleus to another. In view of these limitations, an attempt was made to facilitate the comparison by estimating for each residual nucleus the fraction of each cross section that was missed by the experimental technique and by adjusting each experimental cross section accordingly.

We start with the assumption that an evaporation takes place and determine a reasonable scheme to approximate the initial level population of each residual nucleus. Then, if the decay branching ratios from all levels are known, the fraction f_i

TABLE IX. Comparison of measured cross sections for $\pi^- + {}^{19}F$ with results of an intranuclear cascade/evaporation calculation.

Residual nucleus	Excited state i	α_i[a] (mb)	f_i[a]	$\frac{\alpha_i}{f_i}$[a] (mb)	Bertini/Blann[b] (mb)	$\sum\sigma$[c] (mb)
$^{19}_{9}F$					21.5	28.2[d]
$^{18}_{9}F$	I	21.7	0.53	41	100	43.3
	II	11.6	0.11	108		
	III	4.6	0.050	91		
	V	4.1	0.059	70		
	VI	7.7	0.11	73		
	VII	1.6	0.049	32		
$^{18}_{8}O$	I	23.7	0.88	27	43.7	23.7
	II	1.9	0.31	6.1		
	III	8.3	0.055	150		
	V	7.5	0.062	120		
$^{17}_{9}F$	I	4.0	0.14	28	17.5	4.0
$^{17}_{8}O$	I	20.1	0.25	80	50.1	20.1
$^{17}_{7}N$	I	<3.7	0.39	<9.5	13.4	
$^{16}_{8}O$	II	8.5	0.49	17	27.7	8.5
$^{15}_{8}O$	II	1.1	0.63	1.7	8.7	1.1
$^{15}_{7}N$	I	7.8	0.46	17	27.4	7.8
$^{15}_{6}C$	I	1.7	0.75	2.3	5.0	1.7
$^{14}_{7}N$	I	8.7	0.29	29	16.5	10.5
	IV	2.1	0.28	7.4		
	VI	1.1	0.18	6.1		
$^{13}_{6}C$	II	1.8	0.45	4.1	18.8	3.5
	III	2.7	0.43	6.3		
$^{12}_{6}C$	I	39.8[e]	0.83	48[e]	19.3	39.8[e]

[a] See Sec. IV D for explanation.

[b] An intranuclear cascade/evaporation calculation in which the Bertini code MECC7 (Ref. 32) was used for the cascade phase and Blann-Plasil evaporation code (Ref. 37) for the subsequent evaporation phase; $E_\pi = 220$ MeV.

[c] Sum of measured cross sections for all states of the particular residual nucleus; $E_\pi = 235$ MeV.

[d] Cross section should be considered an upper limit due to possible contributions from secondary neutrons.

[e] Cross section may be contaminated up to 25% by π^- interactions on ^{12}C in the scintillation counters.

TABLE X. Comparison of measured cross sections for $\pi^- + {}^{27}$Al with results of intranuclear cascade/evaporation calculations.

Residual nucleus	Excited state i	α_i [a] (mb)	f_i [a]	$\frac{\alpha_i}{f_i}$ [a] (mb)	Harp *et al.* [b] (mb)	Bertini *et al.* [c] (mb)	$\sum\sigma$ [d] (mb)
$^{27}_{13}$Al					19.6	20.6	100.8 [e]
$^{27}_{12}$Mg					1.9	2.5	1.7 [e]
$^{26}_{13}$Al	II	10.1	0.42	24	78.6	80.2	34.0
	III	19.4	0.26	73			
	VI	5.1	0.076	67			
	X	4.3	0.052	83			
$^{26}_{12}$Mg	I	43.9	0.93	47	33.4	36.6	45
	II	11.5	0.40	29			
$^{25}_{13}$Al	I	<1.6	0.35	<4.5	8.9	9.9	
$^{25}_{12}$Mg	I	6.1	0.33	19	47.2	65.8	24.8
	II	6.2	0.30	20			
	III	13.9	0.22	65			
	VIII	10.2	0.10	99			
$^{25}_{11}$Na	II	<3.7	0.16	<23	4.1		
$^{24}_{12}$Mg	I	33.5	0.72	46	39.2	50.6	33.5
	II	4.7	0.23	21			
$^{24}_{11}$Na	III	3.9	0.095	41	23.6	1.2	3.9
$^{24}_{10}$Ne	II	<6.0	0.16	<36	0.42	4.5	
$^{23}_{12}$Mg	I	<2.1	0.65	<3.2	3.2	2.1	
$^{23}_{11}$Na	I	20.7	0.61	34	42.2	30.4	20.7
$^{23}_{10}$Ne	II	<2.2	0.20	<11	3.1		
$^{22}_{12}$Mg	I	<1.1	0.93	<1.2	0.1		
$^{22}_{11}$Na	III	3.6	0.11	32.7	28.9	35.4	3.6
$^{22}_{10}$Ne	I	15.9	0.96	17	13.9		15.9
$^{21}_{11}$Na	I	0.7	0.65	1.1	3.8		0.7
$^{21}_{10}$Ne	I	13.2	0.76	17	34.9	22.2	13.2
$^{21}_{9}$F	III	<4.5	0.21	<21	1.9	51.4	
$^{20}_{10}$Ne	I	14.7	0.95	15	19.1	5.4	14.7
$^{20}_{9}$F	I	3.3	0.29	11	12.6	0.4	3.3
$^{19}_{10}$Ne	III	<2.1	0.33	<6.3	1.6		
$^{19}_{9}$F	III	5.4	0.25	22	15.1	2.5	5.4
$^{18}_{10}$Ne	II	2.1	0.43	4.9			2.1
$^{18}_{9}$F	I	3.9	0.53	7.3	7.5	3.7	3.9
$^{18}_{8}$O	II	<1.5	0.31	<4.8	5.4		
$^{17}_{9}$F	I	<0.6	0.14	<4.2	1.4		

TABLE X. *(Continued)*

Residual nucleus	Excited state i	α_i [a] (mb)	f_i [a]	$\frac{\alpha_i}{f_i}$ (mb)	Harp *et al.* [b] (mb)	Bertini *et al.* [c] (mb)	$\sum\sigma$ [d] (mb)
$^{17}_{8}$O	I	<4.5	0.25	<18	11.9		
$^{16}_{8}$O	II	7.3	0.49	15	23.5	21.0	7.3
$^{15}_{8}$O	II	<0.5	0.63	<0.8	3.0	3.7	
$^{15}_{7}$N	I	2.0	0.46	4.4	29.1	6.6	2.0

[a] See Sec. IV D for explanation.
[b] See Ref. 38; $E_\pi = 200$ MeV.
[c] See Ref. 39; $E_\pi = 200$ MeV.
[d] Sum of measured cross sections for all states of the particular residual nucleus; $E_\pi = 230$ MeV.
[e] Cross section should be considered an upper limit due to possible contributions from secondary neutrons.

of the total cross section for that residual nucleus which will cascade down to the i^{th} level can be calculated. We then estimate the total cross section for production of that residual nucleus by dividing the measured cross section for the i^{th} level (σ_i) by f_i. If several levels of the same residual nucleus were detected, then σ_i/f_i calculated in this manner should have the same value for each level.

If the processes resulting in the residual nuclei were entirely evaporative, then the initial level population should be proportional to $2J+1$, where J is the spin of the level. According to the INC/E calculation for $\pi^- + {}^{19}$F, the percentage of each residual nucleus produced by evaporation changes gradually with increasing ΔA from less than 2% for ^{18}F to 68% for ^{16}O and to more than 99% for ^{13}C. It is difficult to estimate the correct initial level population for nonevaporative production except for single nucleon removal where direct reaction spectroscopic factors are known. Therefore, it was simply assumed that the initial level population was proportional to $2J+1$ in all cases. We were limited to states for which decay branching ratios were available,[22,23] i.e. generally 10 to 20 states per residual nucleus. Making reasonable averages where ambiguities exist in the published data, we calculated f_i for each residual state for which a cross section had been measured. The resulting values of σ_i/f_i are shown in Tables IX and X for $\pi^- + {}^{19}$F and for $\pi^- + {}^{27}$Al, respectively, and are compared with the INC/E calculation results.

An alternative to this scheme for estimating the missing cross section is to simply sum the cross section σ for various states of each residual nucleus. These values, $\sum\sigma$, were obtained from Tables I and II and are presented in the last column of Tables IX and X. These values are generally lower than the code predictions, especially for the odd mass residual nuclei. A comparison was not made for the $\pi^- + {}^{51}$V results because of the ambiguities in the γ decay schemes of some of the residual nuclei in that case.[23,24]

The uncertainties in σ_i are typically ~20%. Errors in f_i cannot be estimated because f_i is calculated under the assumption that excited states of residual nuclei are populated by an evaporative process resulting in a statistical initial population of states. In an actual evaporation, one might ex-

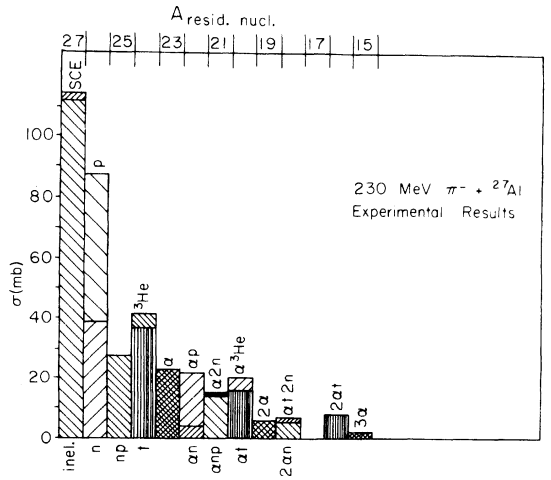

FIG. 5. Removed mass spectrum for $\pi^- + {}^{27}$Al, experimental results. The symbols t, ^{3}He, and α stand for the appropriate clusters or the equivalent nucleons. The experimental results ($\sum\sigma$, Table X) include only formation of excited states from which γ transitions were observed.

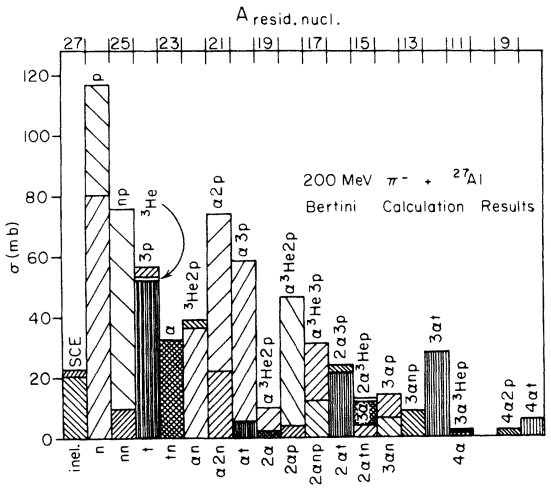

FIG. 6. Removed mass spectrum for $\pi^- + {}^{27}$Al, INC/E calculation results (Bertini). The symbols t, ^{3}He, and α stand for the appropriate clusters or the equivalent nucleons. The calculated cross sections include formation of all bound residual nucleus states. Cross sections smaller than 0.9 mb are not shown.

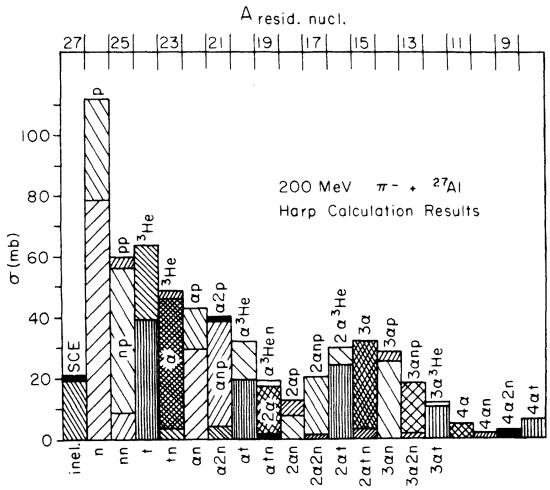

FIG. 7. Removed mass spectrum for $\pi^- + {}^{27}$Al, INC/E calculation results (Harp). The symbols t, ^{3}He, and α stand for the appropriate clusters or the equivalent nucleons. The calculated cross sections include formation of all bound residual nucleus states. Cross sections smaller than 0.9 mb are not shown.

pect that those bound states near the particle instability region would be populated more strongly than lower-energy states. In the present treatment, however, higher-energy bound states are often neglected because their decay schemes are not known. This does not necessarily invalidate the procedure since the γ decay of these highly excited states will feed lower states which are included in the calculations. It was found that values of f_i are relatively insensitive to changes in the initial population assumptions used in the calculation. It should be noted that the closer f_i is to unity (generally true for even-even nuclei) the smaller the uncertainty in α_i/f_i.

If one adds up all values of σ_i/f_i for single and multiple nucleon removal (forming an average for those residual nuclei where more than one state was detected), the results are 359 mb for ^{19}F and 406 mb for ^{27}Al. Both of these values are less than the total single and multiple nucleon removal cross sections calculated by the INC/E codes, indicating that the missing cross section has not been overestimated.

The most exacting test of our procedure would be to compare the values of σ_i/f_i for different states of the same residual nucleus which should be equal if the assumed initial population mechanism is correct. Such a comparison seems to indicate that the initial population assumption is not holding well in these cases. On the other hand, half of the residual nuclei for which this comparison can be made correspond to $\Delta A = 1$, where the codes predict that production occurs predominantly in the cascade phase, so that an initial population scheme based on an evaporation assumption would not be expected to hold well.

While there is no one-to-one correspondence between the α_i/f_i values and the INC/E results shown in Tables IX and X, the overall agreement is sufficiently good to support the hypothesis that the reactions generally proceed by a two-step process as assumed in the calculations, i.e., by a cascade followed by evaporation. The discrepancies between the Harp and Bertini results for ^{27}Al (Table X) apparently reflect the differences in detail[34] between the two codes.

The experimental and INC/E removed mass spectra for $\pi^- + {}^{27}$Al are shown in the form of histograms in Figs. 5, 6, and 7, respectively. The $\Delta A > 4$ cross sections are seen to be smaller relative to the $\Delta A \leq 4$ cross sections in the experimental removed mass spectrum than in both calculated mass spectra, but the Harp calculation appears to represent the observed overall systematics better than the Bertini code. The observed cutoff at $\Delta A = 15$ and some of the other differences in the details of observed and calculated mass spectra may be due to previously discussed limitations of the experimental and computational techniques.

E. Summary

Cross sections for equivalent α removal from the odd-Z–even-N targets studied in this work are considerably smaller than for previously studied even-Z–even-N targets and somewhat

smaller than predicted by the INC/E calculations. Cross sections for equivalent t and $t+n\alpha$ removal, on the other hand, are considerably larger than for even-Z–even-N targets and also larger than predicted by INC/E calculations.

The removed mass spectrum for 235 MeV $\pi^- + {}^{19}F$ for ΔA greater than 2 is similar to that for stopped $\pi^- + {}^{19}F$. This observation is in general agreement with the INC/E prediction that approximately a third of all 220 MeV $\pi^- + {}^{19}F$ interactions result in absorption. Since recent work has indicated that π^- absorption on multinucleon clusters plays an important role,[43] this mechanism may have to be included in the INC/E codes to improve agreement with experiment.

The INC/E calculations predict that single nucleon removal proceeds to a large extent by quasifree scattering. Experimental evidence that pion-induced single nucleon removal may have a significant quasifree component has been noted previously in the resonance behavior displayed by the cross sections (see, e.g., Refs. 10–16) and in the strong production of single-hole states of ^{15}O and ^{15}N in $\pi^\pm + {}^{16}O$ reactions.[7,8] In the present experiment, a comparison between the measured cross sections and direct reaction spectroscopic factors was inconclusive for ^{19}F and ^{51}V because of uncertainties in the effects of γ feeding from higher-energy states. For ^{27}Al, there were clear discrepancies between measured cross sections and spectroscopic factors.

The results obtained on multiple nucleon removal reactions with odd-Z–even-N nuclei give further support to the working hypothesis that has evolved from the interpretation of previous results, mostly on even-Z–even-N nuclei, i.e. that such interactions preferentially occur in two steps. An initial interaction (absorption or nonelastic scattering) results in emission of one or several nucleons and/or in nuclear excitation and is followed by evaporation of additional nucleons and/or nucleon clusters. Because of limitations in the experimental and computational methods used in the present and in previous work, this hypothesis needs to be subjected to further tests, e.g., determination of γ ray and removed particle spectra in coincidence with outgoing particles and inclusion of additional reaction mechanisms in the INC/E codes.

ACKNOWLEDGMENTS

We acknowledge the help of the SREL staff and of J. Batterson in the experimental runs and of M. Jokl in the computer calculations. We are indebted to G. D. Harp and H. W. Bertini for supplying us with results of their computer calculations, to F. Plasil and H. W. Bertini for providing us with copies of their codes, and to N. S. Wall for valuable discussions.

---

*Work supported in part by the National Science Foundation, the National Aeronautics and Space Administration, and the Southern Regional Education Board.

†Present address: Department of Physics, University of South Carolina, Columbia, South Carolina, 29208.

[1]W. J. Kossler, H. O. Funsten, B. A. MacDonald, and W. F. Lankford, Phys. Rev. C 4, 1551 (1971).

[2]P. D. Barnes, R. A. Eisenstein, W. C. Lam, J. Miller, R. B. Sutton, M. Eckhause, J. Kane, R. E. Welsh, D. A. Jenkins, R. J. Powers, R. Kunselman, R. P. Redwine, R. E. Segel, and J. P. Schiffer, Phys. Rev. Lett. 29, 230 (1972).

[3]H. E. Jackson, L. Meyer-Schützmeister, T. P. Wangler, R. P. Redwine, R. E. Segel, J. Tonn, and J. P. Schiffer, Phys. Rev. Lett. 31, 1353 (1973).

[4]V. G. Lind, H. S. Plendl, H. O. Funsten, W. J. Kossler, B. J. Lieb, W. F. Lankford, and A. J. Buffa, Phys. Rev. Lett. 32, 479 (1974).

[5]D. Ashery, M. Zaider, Y. Shamai, S. Cochavi, M. A. Moinester, A. I. Yavin, and J. Alster, Phys. Rev. Lett. 32, 943 (1974).

[6]H. Ullrich, E. T. Boschitz, H. D. Engelhardt, and C. W. Lewis, Phys. Rev. Lett. 33, 433 (1974).

[7]B. J. Lieb and H. O. Funsten, Phys. Rev. C 10, 1753 (1974).

[8]B. J. Lieb, H. S. Plendl, H. O. Funsten, W. J. Kossler, and C. E. Stronach, Phys. Rev. Lett. 34, 965 (1975).

[9]H. E. Jackson, D. G. Kovar, L. Meyer-Schützmeister, R. E. Segel, J. P. Schiffer, S. Vigdor, T. P. Wangler, R. L. Burman, D. M. Drake, P. A. M. Gram, R. P. Redwine, V. G. Lind, E. N. Hatch, O. H. Otteson, R. E. McAdams, B. C. Cook, and R. B. Clark, Phys. Rev. Lett. 35, 641, 1170 (1975).

[10]D. T. Chivers, E. M. Rimmer, B. W. Allardyce, R. C. Whitcomb, J. J. Domingo, and N. W. Tanner, Phys. Lett. 26B, 573 (1968); Nucl. Phys. A126, 129 (1969).

[11]H. S. Plendl, D. Burch, K. A. Eberhard, M. Hamm, A. Richter, C. J. Umbarger, and W. P. Trower, Nucl. Phys. B44, 413 (1972).

[12]K. R. Hogstrom, B. W. Mayes, L. Y. Lee, J. C. Allred, C. Goodman, G. S. Mutchler, C. R. Fletcher, and G. C. Phillips, Nucl. Phys. A215, 598 (1973).

[13]P. J. Karol, A. A. Caretto Jr., R. L. Klobuchar, D. M. Montgomery, R. A. Williams, and M. V. Yester, Phys. Lett. 44B, 459 (1973).

[14]M. A. Moinester, M. Zaider, J. Alster, D. Asheri, S. Cochavi, and A. L. Yavin, Phys. Rev. C 8, 2039 (1973).

[15]M. Zaider, J. Alster, D. Ashery, S. Cochavi, M. A. Moinester, and A. I. Yavin, Phys. Rev. C 10, 938 (1974).

[16]B. J. Dropesky, G. W. Butler, C. J. Orth, R. A. Williams, G. Friedlander, M. A. Yates, and S. B. Kaufman, Phys. Rev. Lett. 34, 821 (1975).

[17]P. J. Castleberry, L. Coulson, R. C. Minehart, and K. O. H. Ziock, Phys. Lett. 34B, 57 (1971).
[18]A. Doron, J. Julien, M. A. Moinester, A. Palmer, and A. I. Yavin, Phys. Rev. Lett. 34, 485 (1975).
[19]C. C. Chang, N. S. Wall, and Z. Fraenkel, Phys. Rev. Lett. 33, 1493 (1974).
[20]V. G. Lind, H. O. Funsten, H. S. Plendl, W. F. Lankford, and A. J. Buffa, Bull. Am. Phys. Soc. 17, 918 (1972); B. J. Lieb, W. F. Lankford, S. H. Dam, H. O. Funsten, W. J. Kossler, H. S. Plendl, V. G. Lind, and A. J. Buffa, *ibid.* 19, 594 (1974).
[21]V. G. Lind, H. S. Plendl, and H. O. Funsten, in Proceedings of Summer School on the Theory of Pion-Nucleus Scattering, Los Alamos, 23–26 July 1973, edited by W. R. Gibbs and B. F. Gibson [Los Alamos Report No. LA-5443-C, 1973 (unpublished)], p. 212.
[22]T. Lauritsen and F. Ajzenberg-Selove, Nucl. Phys. 78, 1 (1966); F. Ajzenberg-Selove and T. Lauritsen, *ibid.* A114, 1 (1968); F. Ajzenberg-Selove, *ibid.* A152, 1 (1970); A166, 1 (1971); A190, 1 (1972).
[23]P. M. Endt and C. van der Leun, Nucl. Phys. A214, 1 (1973).
[24]Nuclear Data Group, *Nuclear Level Schemes A=45 through A=257 from Nuclear Data Sheets* (Academic, New York, 1973); results for ^{50}V were taken from D. G. Rickel and J. D. McCullen, Phys. Rev. C 9, 1446 (1974).
[25]W. J. Kossler, J. Winkler, and C. D. Kavaloski, Phys. Rev. 177, 1725 (1969).
[26]C. W. Lewis, Nucl. Instrum. Methods 123, 289 (1975).
[27]N. P. Jacob and S. S. Markowitz, Phys. Rev. C 13, 754 (1976).
[28]T. Engeland and P. J. Ellis, Nucl. Phys. A181, 368 (1972).
[29]H. D. Engelhardt, C. W. Lewis, and H. Ullrich, Nucl. Phys. A258, 480 (1976).
[30]A. Sourkes, H. Ohnuma, and N. M. Hintz, Nucl. Phys. A217, 438 (1973).
[31]E. Newman and J. C. Hiebert, Nucl. Phys. A110, 366 (1968).
[32]H. W. Bertini, Phys. Rev. 131, 1801 (1963); Phys. Rev. C 6, 631 (1972).
[33]G. D. Harp, K. Chen, G. Friedlander, Z. Fraenkel, and J. M. Miller, Phys. Rev. C 8, 581 (1973).
[34]H. W. Bertini, G. D. Harp, and F. E. Bertrand, Phys. Rev. C 10, 2472 (1974).
[35]V. S. Barashenkov, H. W. Bertini, K. Chen, G. Friedlander, G. D. Harp, A. S. Ilienov, J. M. Miller, and V. D. Toneev, Nucl. Phys. A187, 531 (1972).
[36]K. Garrett and L. Turkevich, Phys. Rev. C 8, 594 (1973).
[37]M. Blann, Nucl. Phys. 80, 223 (1966); M. Blann and F. Plasil, Phys. Rev. Lett. 29, 303 (1972); S. Cohen, F. Plasil, and W. J. Swiatecki, Ann. Phys. 82, 557 (1974).
[38]G. D. Harp (private communication).
[39]H. W. Bertini (private communication).
[40]J. Hüfner, L. Tauscher, and C. Wilkin, Nucl. Phys. A231, 455 (1974).
[41]V. M. Kolybasov, Yad. Fiz. 3, 729 (1966) [Sov. J. Nucl. Phys. 3, 535 (1966)].
[42]H. Nishimura and A. Arima, in Proceedings of the Sixth International Conference on High Energy Physics and Nuclear Structure, Santa Fe, June 1975 (unpublished), p. 173.
[43]J. Comiso, T. Meyer, F. Schlepuetz, and K. O. H. Ziock, Phys. Rev. Lett. 35, 13 (1975).